Journal of Materials Chemistry

Cite this: J. Mater. Chem., 2012, 22, 4502

www.rsc.org/materials

PAPER

Multifunctional electron-transporting indolizine derivatives for highly efficient blue fluorescence, orange phosphorescence host and two-color based white OLEDs

Jing Wan,†[ac] Cai-Jun Zheng,†[ab] Man-Keung Fung,[b] Xiao-Ke Liu,[ac] Chun-Sing Lee*[b] and Xiao-Hong Zhang*[a]

Received 30th September 2011, Accepted 22nd November 2011
DOI: 10.1039/c2jm14904d

In this work, derivatives of indolizine are first used as electron-transporting host materials for hybrid fluorescence/phosphorescence white organic light-emitting devices (F/P-WOLED). Of the indolizine derivatives, a blue fluorescent material **BPPI** (*3-(4,4′-biphenyl)-2-diphenylindolizine*) was found to have: (1) blue emission with high quantum yields, (2) good morphological and thermal stabilities, (3) electron-transporting properties, and (4) a sufficiently high triplet energy level to act as a host for red or yellow-orange phosphorescent dopants. The multifunctional **BPPI** enables adaptation of several simplified device configurations. For example, a non-doped blue fluorescent device exhibits good performance with an external quantum efficiency of 3.16% and Commission Internationale de l'Eclairage coordinates of (0.15, 0.07). A high-performance orange phosphorescent device was found to have a high current efficiency of 23.9 cd A^{-1}. Using **BPPI**, we also demonstrate a F/P-WOLED with a simplified structure, stable emissions and respectable performance (current and external quantum efficiencies of 17.8 cd A^{-1} and 10.7%, respectively).

Introduction

Lighting takes up a significant part of the energy resources of the world, with a large share still consumed by inefficient incandescent lamps. White organic light-emitting diodes (WOLEDs) show promise in future ambient lighting applications due to their favorable properties, including homogenous large-area emission, good color rendering and potential realization on flexible substrates, which also opens new areas in lighting design, such as light ceilings or luminous objects of almost any shape.[1] At present, WOLEDs already find application in color flat panel displays; however, in the illuminant and lighting domains, the performance characteristics (*e.g.*, efficiency and lifetime) of WOLEDs are still not adequate.

Materials are vital components of OLEDs. At present, searching for high performance materials has gained increasing attention, driving the further development of OLEDs. In 2006, Forrest *et al.* proposed a hybrid fluorescent/phosphorescent route to realize efficient WOLEDs.[2] In this design, the emitting layer should not only show highly efficient blue fluorescence, but also sensitize the green, red or yellow-orange phosphors. However, as the structure of OLED devices has become increasingly complicated, the material requirements have also become more critical. For these new F/P-WOLEDs, the host materials play a significant role and generally should have high blue luminous efficiencies and suitable triplet state levels. So far, there are limited numbers of molecular systems fulfilling these requirements.[2–11]

Recently, we have found that indolizine derivatives, which have never been applied to OLEDs, possess the following novel properties:[12,13] (1) blue emissions with high quantum yields, (2) electron-transporting properties, and (3) sufficiently high triplet energy (E_T) levels. These demonstrate that indolizine derivatives have the potential to be good host materials in F/P-WOLEDs. Therefore, in this work, we designed, synthesized and characterized the following indolizine derivatives: *1,4-di-3′-(2′-phenylindolizyl)-benzene* (**PPI**), *1,4-di-3′-(2′-naphthalenylindolizyl)-benzene* (**PNI**), *3-(4,4′-biphenyl)-2-diphenylindolizine* (**BPPI**), *3-(4,4′-biphenyl)-2-dinaphthalenylindolizine* (**BPNI**), *1,3,5-tri[4-3′-(2′-naphthalenylindolizyl)phenyl]benzene* (**p-TPPNI**) and *1,3,5-tri[3-3′-(2′-phenylindolizyl)phenyl]benzene* (**m-TPPPI**), with the aim of clarifying the relationships between their properties and molecular structures. Each of the above compounds consists of two to three indolizine cores linked together with different phenyl bridging groups (Scheme 1). The phenyl linking groups are expected to enhance the light-emitting efficiency by providing an extended conjugated structure and increasing the number of

[a]*Nano-organic Photoelectronic Laboratory and Key Laboratory of Photochemical Conversion and Optoelectronic Materials, Technical Institute of Physics and Chemistry, Chinese Academy of Sciences, Beijing, 100190, China. E-mail: xhzhang@mail.ipc.ac.cn*
[b]*Center of Super-Diamond and Advanced Films (COSDAF) and Department of Physics and Materials Science, City University of Hong Kong, Hong Kong SAR, China. E-mail: apcslee@cityu.edu.hk*
[c]*Graduate University of Chinese Academy of Sciences, Beijing, 100039, China*
† These authors contributed equally to this work

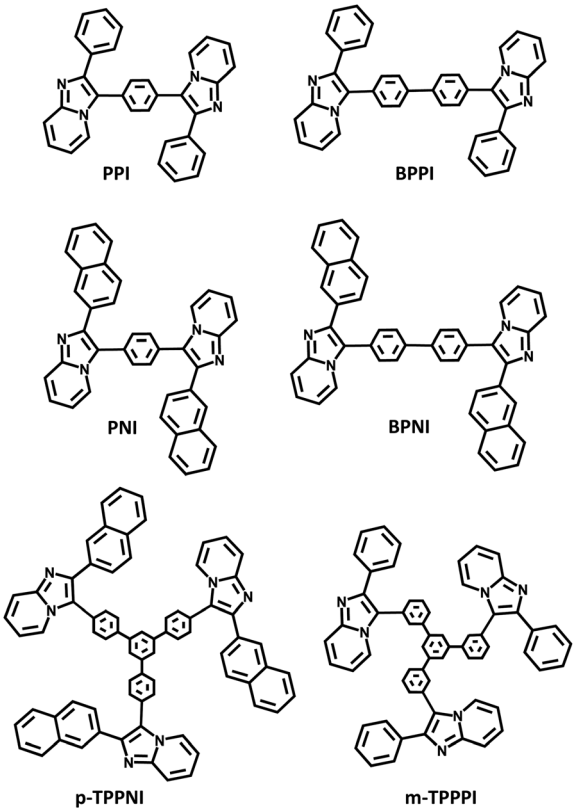

Scheme 1 Molecular structures of the indolizine derivatives.

indolizine units. In addition, bulky phenyl groups can further increase steric hindrance and cause molecular non-planarity and result in better thermal stability. Due to the electron-deficient nitrogen-containing heterocyclic moieties in the indolizine cores, the materials have natural electron-transporting properties.[14,15,16] Meanwhile, the attachment of indolizine groups at the 2-position also leads to amorphous materials.[12a] Of these materials, we found that **BPPI** has high blue fluorescent efficiency, reasonable electron-transport properties, good thermal stability, and suitable triplet state energy levels. Based on this multifunctional material, blue fluorescent, orange phosphorescent devices as well as F/P-WOLEDs with simplified structures were fabricated and shown to have remarkable performances.

Results and discussion

Synthesis and characterization

As shown in Scheme 2, the 6 blue fluorescent materials were synthesized from iodo-substituted species, 3-iodo-2-phenylindolizine and 3-iodo-2-naphthalenylindolizine, which were obtained as reported in literature.[14,17] Firstly, 2-bromoacetophenone and 2-bromoacetonaphthone were successfully obtained by the bromination of acetophenone and acetonaphthone with NBS.[17] Secondly, 2-phenylindolizine and 2-naphthalenylindolizine were readily prepared in good yields (67% and 87%) from 2-bromoacetophenone and 2-aminopyrididine and the corresponding 2-bromoacetophenones.[13] Thirdly, 3-iodo-2-phenylindolizine (**1**) and 3-iodo-2-naphthalenylindolizine (**2**) were easily obtained by the iodination of

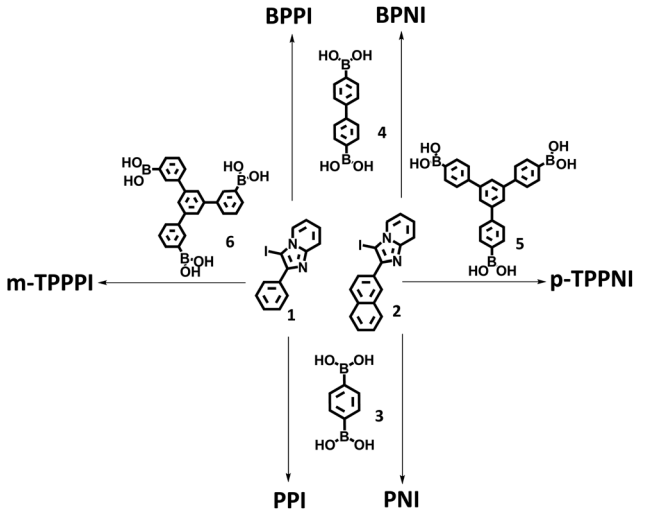

Scheme 2 Synthesis of the indolizine derivatives. Reagent: $Pd(PPh_3)_4$, NaOH (aq. 2M), DME, 40 h, 85 °C.

2-phenylindolizine and 2-naphthalenylindolizine with excess iodine.[13] In addition, the dibromo-aromatic compounds and tribromo-aromatic compounds reacted readily with *n*-butyl lithium in dry tetrahydrofuran at −78 °C to form the corresponding difunctional or trifunctional lithium reagents, resulting in satisfactory yields (35%–60%) of the corresponding boronic acids (**3–6**) when treated with ethereal trimethyl borate at −78 °C, with subsequent acidification.[18] Then, the Suzuki-cross coupling of 3-iodo-2-phenylindolizine (**1**) and 3-iodo-2-naphthalenylindolizine (**2**) with the corresponding boronic acids resulted in all 6 blue fluorescent materials producing moderate to ideal yields.[13,19]

All the blue emitters were fully characterized by ^{1}H NMR, fast atom bombardment or electron impact-mass spectrometry (FAB-MS or EI-MS), and were consistent with the proposed structures. All the data are given in the Experimental section.

Thermal properties

Thermal properties of the newly synthesized compounds were examined by thermogravimetric analysis (TGA) and differential scanning calorimetry (DSC) in a nitrogen atmosphere at a scanning rate of 10 K min^{-1}. All the materials revealed good thermal stabilities, with a 5% weight loss at temperatures (T_D) exceeding 385 °C, as determined by TGA measurements. Key thermal properties including T_D, melting temperatures, T_m, and glass-transition temperatures, T_g, of the compounds are summarized in Table 1. It can be seen that T_D can be increased by replacing the phenyl group with a naphthyl group at the 2-position of the indolizine unit or by increasing the size of the linking group between the indolizine units. The compounds (except **BPPI** and **BPNI**) also show T_g values greater than 170 °C. Probably due to their bulky structures, T_g in **BPPI** and **BPNI** were not observed. The good thermal properties of the compounds are advantageous for application as host materials in OLEDs. This is because in a morphologically stable amorphous host material, the emitter molecules are homogenously diluted, thus minimizing concentration quenching.[20]

Table 1 Thermal, photophysical and electrochemical properties as well as energy levels of the six indolizine derivatives

	$T_m/T_D/T_g$ [°C][a]	λ_{abs}, CH_2Cl_2 [nm] [b]	λ_{em} (Φ_f), CH_2Cl_2 [nm (%)] [c]	λ_f, film [nm][c]	λ_p (E_T), 77 K [nm (eV)][d]	ΔE_g [eV][e]	E_{OX} [eV][f]	HOMO/LUMO [eV][g]
PPI	280/389/175	334.3	411.2 (53.02%)	435	475 (2.62)	3.20	1.263	5.52/2.32
PNI	292/408/184	337.8	425.4 (43.08%)	444	511 (2.42)	3.17	1.285	5.54/2.37
BPPI	348/414/—	338.3	414.4 (83.00%)	430	478 (2.59)	3.19	1.285	5.54/2.35
BPNI	326/463/—	343.4	423.6 (66.15%)	437	506 (2.45)	3.17	1.293	5.55/2.38
p-TPPNI	294/507/187	330.2	410.7 (41.70%)	398	503 (2.47)	3.23	1.293	5.55/2.32
m-TPPPI	279/492/186	314.8	399.4 (37.93%)	404	507 (2.45)	3.21	1.349	5.61/2.40

[a] T_D: Decomposition temperatures, observed in a thermogravimetric experiment with a heating rate of 10 K min^{-1} in a nitrogen atmosphere. T_m: Melting temperatures, T_g: Glass transition temperatures. [b] λ_{abs}: Absorption maximum. [c] λ_{em}: Emission maxima were measured both in solution and in thin films. The quantum yields (Φ_f) were measured in dichloromethane solution, see ref. [21]. [d] λ_p: Phosphorescence emission peak and E_T: Triplet energy measured in 2-methyltetrahydrofuran at 77 K. [e] ΔE_g: The band-gap energies were estimated from the optical absorption edges of solid films on quartz substrates. [f] E_{OX}: Electrochemical first oxidation potentials with respect to the ferrocene/ferrocenium redox potential, which is 0.4825 eV *vs.* SCE, determined by differential pulse voltammetry in a 0.1 M solution of $TBAPF_6$ in dichloromethane. [g] HOMO = $-E_{OX}$ (*vs* SCE) − E_{SCE} and LUMO = HOMO + ΔE_g, the energy level of SCE (E_{SCE}) is 4.74 eV *vs.* vacuum level.[22]

Photophysical properties

Absorption and emission spectra of these blue emitters were studied in dichloromethane and solid film. Table 1 indicates that the absorptions are only mildly sensitive to the molecular structure. In the first four compounds, slight red shifts in the absorption (λ_{abs} value) were observed when the extent of molecular conjugation was increased by replacing the phenyl groups with naphthyl groups at the 2-position of the indolizine units (**PNI** > **PPI** and **BPNI** > **BPPI**) or by using a diphenyl instead of a phenyl group for bridging the indolizine units (**BPPI** > **PPI** and **BPNI** > **PNI**). On the other hand, using a star-shaped four benzene bridging group would hinder conjugation between indolizine units, resulting in blue-shifted absorption in **p-TPPNI** and **m-TPPPI**.

All six compounds show blue or near ultraviolet fluorescence in both solution and solid states. Emission peaks of the compounds show similar trends to the absorption. Key photophysical parameters of the compounds are summarized in Table 1. By using quinine bisulfate as the calibration standard, fluorescence quantum yields of PPI, PNI, BPPI, BPNI, p-TPPNI and m-TPPPI in dichloromethane were determined to be 53.02%, 43.08%, 83.00%, 66.15%, 41.70% and 37.93% respectively. Due to the fact that the electron delocalization ability of the naphthyl moiety is stronger than that of the phenyl moiety, **PPI** and **BPPI** have slightly higher Φ_f values than **PNI** and **BPNI**, respectively. Although some of these values are not high enough to enable application as high performance blue emitters for OLEDs, **BPPI**, whose fluorescence quantum yield reaches a high level of 83.00%, can obviously take this role.

Due to the greater electron delocalization ability and larger π-conjugation plane, naphthyl moieties on the 2-position of the indolizine units are relatively more delocalized than the phenyl moiety and thus increase the extent of π-orbital conjugation within each indolizine unit. In turn, this decreases the π-orbital conjugation between different indolizine units in the whole molecule. This would decrease both Φ_f and the red shift of λ_{em}. On the other hand, the π-orbital conjugation between different indolizine units in the whole molecule increases when there are more bridging phenyl groups between the indolizine units (*e.g.*, biphenyl *vs.* phenyl). This leads to an increase in Φ_f (*e.g.* **BPPI** *vs.* **PPI**, **BPNI** *vs.* **PNI**). In comparison, if the bridging phenyl groups between the indolizine units are star-shaped four benzene ring systems, both Φ_f and λ_{em} decrease. This is due to the fact that the star-shaped bridging group would hinder the conjugation between each indolizine unit.

Phosphorescence spectra of these compounds were also studied (measured at 77 K) (Fig. 1c). The E_T levels of the compounds were estimated by taking the highest energy peak of the phosphorescence as the vibronic 0–0 transition energy of $T_1 \rightarrow S_0$. As shown in Table 1, the E_T levels of all 6 compounds are greater than 2.4 eV. These suggest that the materials should have good potential for application as host materials for red or orange phosphorescent dopants.

Electrochemical properties

Electrochemical properties of the indolizine derivatives were studied by cyclic voltammetry (CV) in a conventional three-electrode cell, using a glassy carbon working electrode, a platinum wire counter electrode, and a saturated calomel electrode (SCE) reference electrode. The oxidation processes were investigated in dichloromethane solution. The highest occupied molecular orbital (HOMO) levels of the compounds were estimated from the first oxidation peak relative to ferrocene. The lowest unoccupied molecular orbital (LUMO) levels were calculated by adding the band gaps (E_g), determined from the optical absorption edges of solid films on quartz substrates, to the HOMO levels (Table 1). It can be seen that **PPI**, **PNI**, **BPPI** and **BPNI** have similar HOMO levels of 5.52, 5.54, 5.54 and 5.55 eV, and LUMO levels of 2.32, 2.37, 2.35 and 2.38 eV, respectively.

OLED characterization

Based on the above, **BPPI** was identified to have the highest potential for application in OLEDs. Using **BPPI**, a blue fluorescent device (device A) with a configuration of indium tin oxide (ITO)/NPB (30 nm)/TCTA (10 nm)/BPPI (30 nm)/LiF (1.5 nm)/Al was fabricated to check whether **BPPI** can be used as a blue emitter. In this device, ITO and LiF/Al served as the anode and the cathodes, respectively; 4,4′-bis[*N*-(1-naphthyl)-*N*-phenyl-amino]biphenyl (NPB) was used as the hole-transporting layer (HTL); and 4,4′,4″-tris(*N*-carbazolyl)triphenylamine (TCTA)

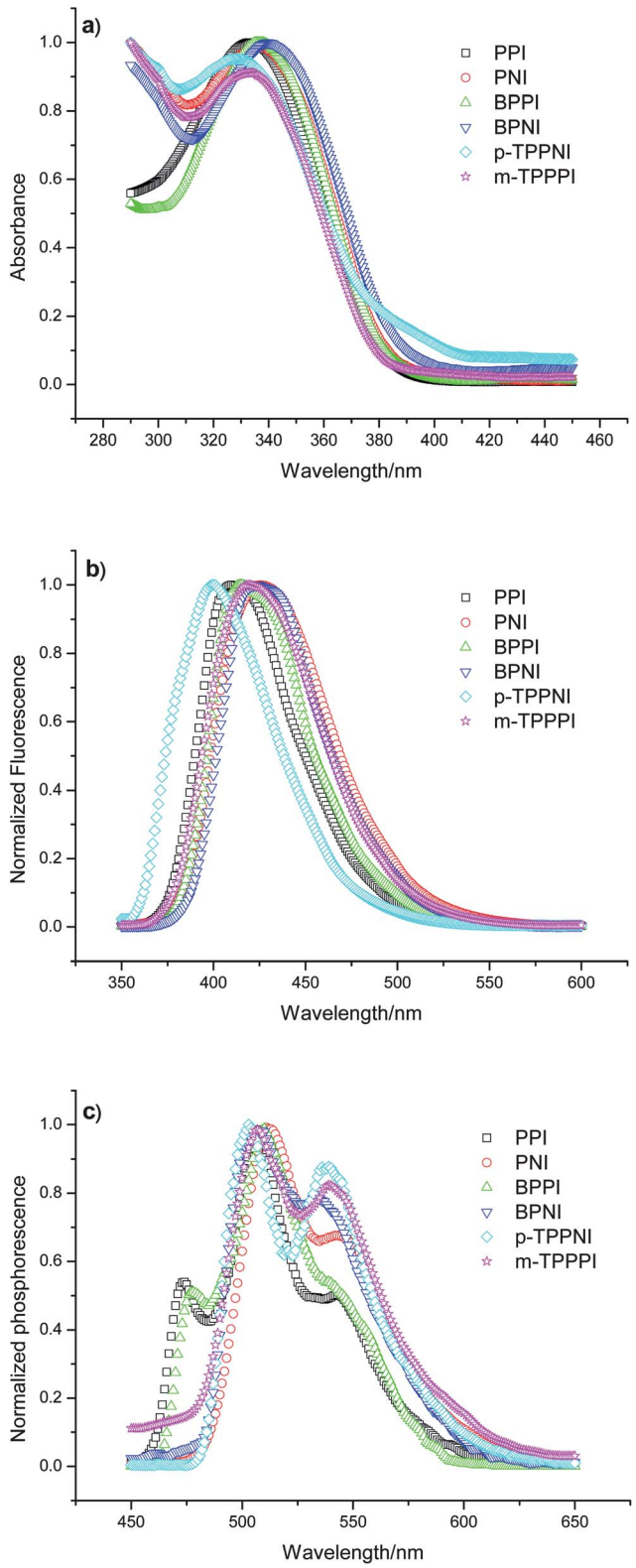

Fig. 1 a) Absorption spectra in dichloromethane solution. b) Emission spectra in dichloromethane solution. c) Phosphorescence emission spectra in 2-methyltetrahydrofuran at 77 K.

was the electron blocking layer (EBL). Considering that the multifunctional compound **BPPI** has both electron-transporting properties and efficient blue emission, we simplified the device structure by using **BPPI** as the electron-transporting layer (ETL) and emitting layer (EML), simultaneously.

As shown in Fig. 2(c), the fluorescent device exhibits stable deep-blue electroluminescence (EL) at different luminances. The Commission Internationale de l'Eclairage (CIE) coordinates of the blue device are (0.15, 0.07), which is very close to the NTSC standard blue color (0.14, 0.08). Fig. 2(b) shows EQE–current density characteristics of the device. The maximum EQE of the blue device is 3.16%, which is a respectable result among blue fluorescent devices.[23,24,25]

To confirm whether **BPPI** can be used as a phosphorescent host, tris(2-phenylquinoline)iridium ($Ir(2\text{-phq})_3$) doped orange phosphorescent device (device B) with a configuration of ITO/NPB (30 nm)/TCTA (10 nm)/BPPI: 2%$Ir(2\text{-phq})_3$ (30 nm)/BPPI (30 nm)/LiF (1.5 nm)/Al, was fabricated. A 60 nm **BPPI** layer was also used as both EML and ETL in this device. From Fig. 2(d), the turn-on voltage of the device is about 4.0 V, and the maximum current density at a driving voltage of 10 V is around 60 mA cm^{-2}. The relatively low current density is probably due to the thick **BPPI** layer, and also the possibly lower electron transporting mobility of **BPPI**, compared to common electron transporting materials, such as TPBI, BCP, *etc.* From Fig. 2(e), the maximum current efficiency of the device is 23.9 cd A^{-1} and shows a mild efficiency roll-off at high current densities. Fig. 2(f) shows the EL spectra of the device at different luminances; the EL spectra only show the $Ir(2\text{-phq})_3$ emission from 10 to 10 000 cd m^{-2}. These confirm that **BPPI** efficiently sensitizes the triplet emission of the orange phosphor.[26,27,28]

The results of the blue fluorescent and the orange phosphorescent devices suggest that BPPI can be used as a host for F/P-WOLEDs. We thus fabricated a white device (device C) with a simplified configuration of ITO/NPB (30 nm)/TCTA (10 nm)/BPPI (10 nm)/BPPI:2%$Ir(2\text{-phq})_3$ (20 nm)/BPPI (30 nm)/LiF (1.5 nm)/Al. Since TCTA and **BPPI** mostly conduct holes and electrons respectively, the main exciton generation zones would be located at the TCTA/BPPI interfaces (Fig. 3). Considering the short diffusion lengths (3 nm) of the singlet excitons, 10 nm undoped **BPPI** spacers were placed to capture the singlet excitons for blue emission. The triplet excitons were then transferred to $Ir(2\text{-phq})_3$ doped in the middle layers for their long diffusion lengths of 100 nm. The high singlet energy level (3.4 eV) and E_T level (2.8 eV) of TCTA confine all excitons, such that they can be used in the EML. The maximum EQE (Fig. 4(b)) of the **BPPI**-based F/P-WOLED is 10.7%.[2,6] This is a respectable result for WOLEDs considering the simplified device structure. The EL spectra at different luminances of the white device are shown in Fig. 4(c), which reveals that the amount of blue emission slightly decreases with increasing current density. The reason for the decrease in blue emission might be that the concentration annihilation between **BPPI** molecules is higher than the triplet–triplet annihilation at high exciton concentrations. At different luminances, the device exhibits white emission. From luminances of 100 to 10 000 cd m^{-2}, the color coordinates are only slightly shifted by (+0.03, +0.03). Electroluminescent data of the devices A–C are shown in Table 2.

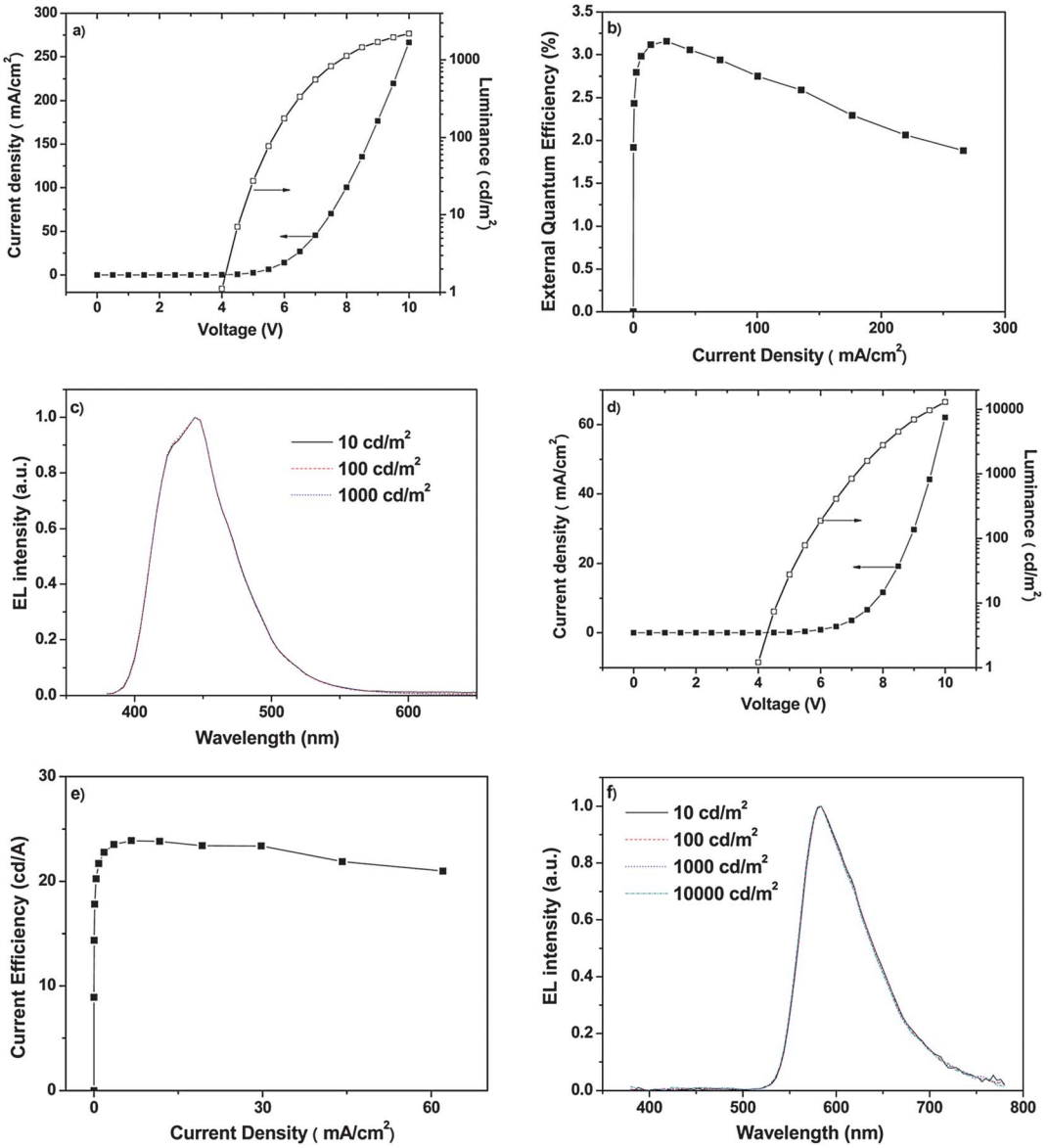

Fig. 2 a), d) Current density and luminance plotted against applied electric field, characteristic for devices A and B. b), e) Current efficiency plotted against current density for devices A and B. c), f) EL spectra for devices A and B at different luminances.

Conclusions

In summary, we synthesized and characterized a series of indolizine derivatives and demonstrated their applications as electron-transporting hosts and deep-blue emitters. To the best of our knowledge, the current work is the first attempt to apply indolizine derivatives in OLEDs. With a systematic variation of the molecular structures and studies of their properties, **BPPI** exhibits the following properties: (1) blue emission with high quantum yields, (2) high morphological and thermal stabilities, (3) electron transporting properties, and (4) a sufficiently high E_T level to act as red or yellow-orange phosphorescent host. Based on this multifunctional compound, the non-doped blue fluorescent device exhibits good performance with an EQE of 3.16% and CIE coordinates of (0.15, 0.07); moreover, the orange phosphorescent device achieves a high current efficiency of 23.9 cd A^{-1}. Finally, the proposed F/P-WOLED with a simplified structure delivers a respectable performance with high efficiency and stable emissions.

Experimental

General methods

The starting materials, 4,4′-dibromobiphenyl, 2,2′-dibromophenyl, 3-bromoacetophenone and 4-bromoacetophenone were purchased from Alfa Asia and used without further purification. All of the arylboronic acids were prepared in two steps from corresponding aryl halides and the final compounds were prepared by using Suzuki-type cross-coupling reactions according to published procedures.[14,15] All of the reactions and manipulations were carried out under N_2 with the use of a standard inert atmosphere and Schlenk techniques. The solvents were dried by standard procedures. All of the

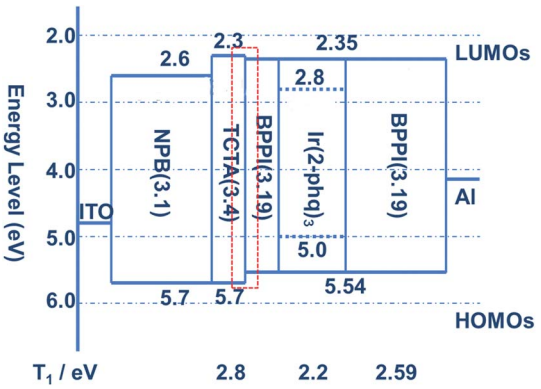

Fig. 3 Energy diagram and device structure of the F/P-WOLED. The numbers in parentheses indicate the energy gaps of materials. T_1: Triplet energy. The red dotted line square zone indicates the exciton formation zone.

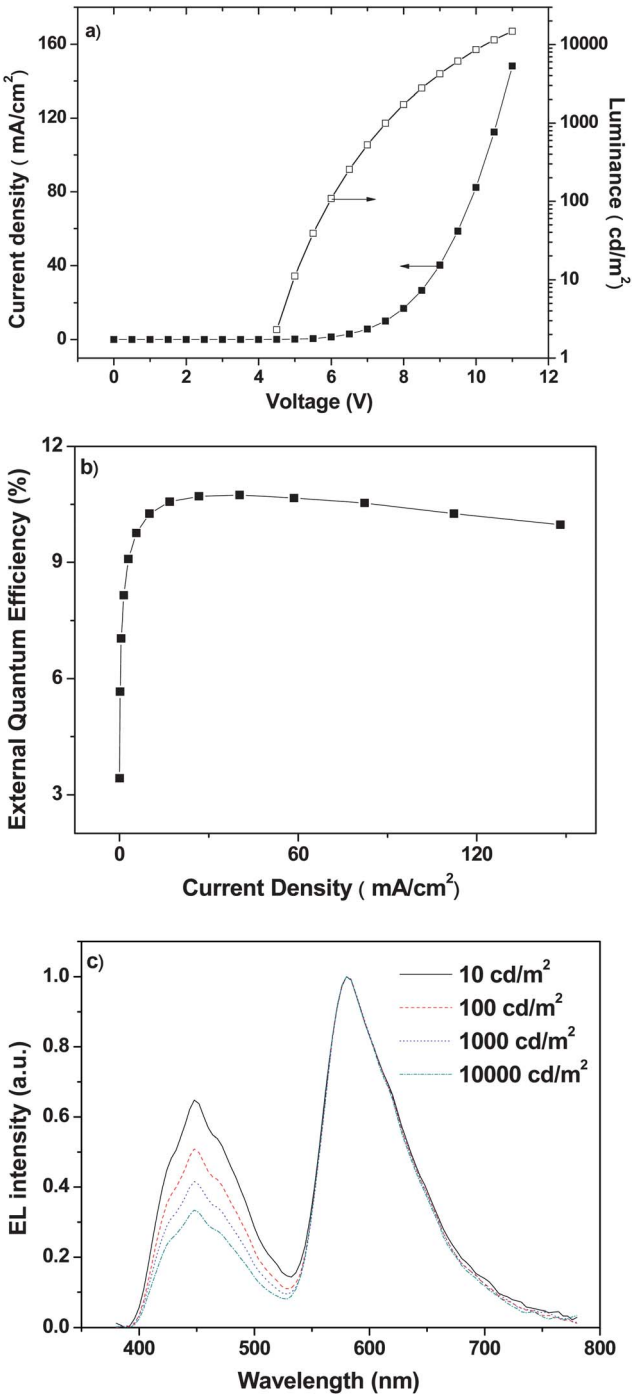

Fig. 4 a) Current density and luminance plotted against applied electric field, characteristic for device C. b) Current efficiency plotted against current density for device C. c) EL spectra for device C at different luminances.

column-chromatography measurements were performed using silica gel (100–200 mesh or 200–300 mesh, Sinopharm Chemical Reagent Co.) as the stationary phase in a column 15–20 cm in length and 2.0 cm–6.0 cm in diameter. The NMR spectra were recorded on Varian-Gemini 300 and Bruker Avance Π-400 spectrometer at room temperature. The electronic absorption spectra were measured using a Hitachi UV-Vis spectrophotometer U-3010. The fluorescence spectra were recorded using a Hitachi fluorescence spectrometer F-4500. The emission quantum yields were measured with reference to quinine bisulfate in 0.1 N sulfuric acid solution.[18] The fluorescence lifetimes of the compounds in solution were determined using a single-photon counting fluorescence lifetime apparatus F900 (Edinburgh Instruments Company). The phosphorescence spectra of the compounds (in the 2-methyltetrahydrofuran solution) were measured using a Hitachi fluorescence spectrometer F-4500 at 77 K. The cyclic voltammetry (CV) experiments were performed using a Potentiostat/Galvanostat Model 283 electrochemical analyzer. All of the measurements were carried out at room temperature with a conventional three-electrode configuration consisting of a glassy carbon working electrode, a platinum wire counter electrode, and a SCE (saturated calomel electrode) reference electrode. The E_{OX} values were determined as electrochemical first oxidation potentials with respect to the ferrocene/ferrocenium redox potential. The solvent in all of the experiments was CH_2Cl_2 and the supporting electrolyte was 0.1 M tetrabutylammonium hexafluorophosphate ($TBAPF_6$). The DSC measurements were carried out using a TA Instruments DSC 2910 thermal analyzer at a heating rate of 10 °C min^{-1}. The TGA measurements were performed on a TA Instruments TGA 2050 thermal analyzer. Low- and high-resolution mass spectra were recorded using a BIFLEXIII MALDI-TOF mass spectrometer in MALDI mode or in EI mode.

Synthesis of 1,3,5-trialkylbenzenes: general procedure. Thionyl chloride (0.8 mL, 11 mmol) was added slowly by a syringe to a stirred solution of bromoacetophenone (1 g, 5 mmol) in anhydrous ethanol (2 mL, 35 mmol). The mixture was stirred for 1 h at reflux temperature and then neutralised with a saturated sodium carbonate solution. The solid obtained on cooling was filtered, washed with cold water, ether and ethanol, and dried under reduced pressure to give the intermediate compound.

1,3,5-Tri(4-bromophenyl)benzene. Light yellowish solid. M.P. 262–263 °C. ^{1}H NMR (400 MHz, $CDCl_3$, 25 °C, TMS) δ 7.69 (s, 3H), 7.59–7.62 (m, 6H), 7.52–7.55 (m, 6H). TOF EI-MS: 543.8333 $[M]^+$.

Table 2 Electroluminescent data of the devices A–C

	V_{on} [V][a]	L_{max} (Voltage) [cd m^{-2} (V)][b]	λ_{em} [nm][c]	CIE @100 cd m^{-2} [x, y][d]	$\eta_{ext,max}$ [%][e]	$\eta_{L,max}$ [cd A^{-1}][f]
Device A	4.00	2204 (10.0)	444	(0.15, 0.07)	3.16	1.25
Device B	4.00	13010 (10.0)	582	(0.55, 0.44)	12.4	23.9
Device C	4.20	14830 (11.0)	446	(0.41, 0.33)	10.7	17.8

[a] V_{on} (turn-on voltage) was obtained from the *x*-intercept of plot of log(luminance) against applied voltage. [b] *L*: Luminance; max: maximum. [c] λ_{em}: Emission wavelength. [d] CIE (x,y): Commission Internationale de l'Eclairage coordinates. [e] η_{ext}: External quantum efficiency; max: maximum. [f] η_L: Current efficiency; max: maximum.

1,3,5-Tri(3-bromophenyl)benzene. Light yellowish solid. M.P. 167–168 °C. ^{1}H NMR (400 MHz, $CDCl_3$, 25 °C, TMS) δ 7.73 (s, 3H), 7.63–7.67 (m, 3H), 7.37–7.43 (m, 6H), 7.25–7.28 (m, 3H). TOF EI-MS: 543.8421 $[M]^+$.

Synthesis of arylboronic acids 3–6: general procedure

*Biphenyl-4,4′-diboronic acid (**4**).*[8,9] *n*-Butyl lithium (1.6 mL, 2.72 M in hexanes; 4.35 mmol) was added dropwise to a solution of 4,4′-dibromo-1,1′-biphenyl (0.5 g, 1.6 mmol) in THF at −78 °C. The solution was stirred for 10 min at −78 °C, and 1 h at room temperature. The mixture was re-cooled to −78 °C and trimethylborate (1.0 mL, 8 mmol) was added rapidly. The mixture was allowed to warm to room temperature and stirred for 16 h before being quenched with aqueous hydrochloric acid (8 mL, 2 M). The solvent was removed in vacuum to give a white residue, which was dissolved in a sodium hydroxide solution (500 mL, 2 M) and filtered. Acidification of the filtrate to pH = 1 with hydrochloric acid (35%) gave a fine, white precipitate, which was collected by centrifugation. The crude diboronic acid **4** was dried and used unpurified in the next step.

Synthesis of 2-bromoacetophenone and 2-bromoacetonaphthone: general procedure. To a mixture of acetophenone **7** (1.17 mL, 10 mmol) and NBS (1.869 g, 10.5 mmol) in dry Et_2O (10 mL) was added NH_4OAc (77.8mg, 1 mmol). After stirring at 25 °C for 0.5 h, the mixture was filtered and the filtrate was washed with water, dried and evaporated. The residue was chromatographed (hexane–acetone = 10 : 1) on silica gel to give the product (92%). 2-bromoacetonaphthone was also prepared from acetonaphthone and NBS by a similar procedure (87%).

Synthesis of indolizines: general procedure. A mixture of 2-aminopyridine (0.58 g, 6.2 mmol), 2-bromoacetophenone (1.0 g, 5.0 mmol), and sodium hydrogen carbonate (0.65 g, 7.8 mmol) in ethanol (10 mL) was stirred for 12 h at room temperature. The solution was evaporated *in vacuo*, and water (50 mL) was added to the residue. This was extracted with chloroform twice (50 mL × 2), and the chloroform solution was washed with water (50 mL) and brine (50 mL). The chloroform solution was dried over sodium sulfate, and the filtrate was evaporated in vacuum. The crude product was subjected to column chromatography on alumina (solvent: dichloromethane) to obtain 2-phenylindolizine (4.3 mmol; 86%). 2-naphthalenylindolizine was also prepared from 2-aminopyridine and 2-bromoacetonaphthone by a similar procedure except for the requirement of higher reaction temperature (80 °C).

2-Phenylindolizine. white beige solid, M.P. 135–136 °C; ^{1}H NMR (400 MHz, $CDCl_3$, 25 °C, TMS) δ 8.13 (d, J = 6.76 Hz, 1H), 7.97 (d, J = 7.4 Hz, 2H), 7.88 (s, 1H), 7.66 (d, J = 9.12 Hz, 1H), 7.44 (t, J = 7.44 Hz, 2H), 7.34 (t, J = 7.36 Hz, 1H), 7.18 (t, J = 7.68 Hz, 1H), 6.79 (t, J = 6.72 Hz, 1H); TOF EI-MS: 194.0582 $[M]^+$.

2-Naphthalenylindolizine. yield 67%, white beige solid, M.P. 155–162 °C; ^{1}H NMR (400 MHz, $CDCl_3$, 25 °C, TMS) δ 8.53 (s, 1H), 8.17 (d, J = 6.9 Hz, 1H), 7.83–8.04 (m, 5H), 7.69 (d, J = 9.0 Hz, 1H), 7.46–7.50 (m, 2H), 7.18–7.26 (m, 1H), 6.81 (t, J = 7.1 Hz, 1H); TOF EI-MS: 244.0681 $[M^+]$.

Synthesis of iodo compounds 1, 2: general procedure for reaction with iodine. To a solution of 2-phenylindolizine (0.50 g, 2.6 mmol) in pyridine (5 mL) was added iodine (1 g, 4 mmol). The reaction mixture was heated at 50 °C for 5 h and then poured into water (50 mL). The aqueous solution was extracted with dichloromethane (30 mL × 3). The combined organic extracts were washed with water (50 mL), $Na_2S_2O_3$ (aq) (50 mL), and brine (50 mL). The dichloromethane solution was dried over sodium sulfate, and the filtrate was evaporated in vacuo. The crude product was subjected to column chromatography on alumina (solvent: dichloromethane) to obtain **1** (2.2 mmol; 84%)

*3-Iodo-2-phenylindolizine (**1**).* pale yellow solid, M.P. 169–171 °C; ^{1}H NMR (400 MHz, $CDCl_3$, 25 °C, TMS) δ 8.27 (d, J = 6.84 Hz, 1H), 8.08 (d, J = 7.4 Hz, 2H), 7.63 (d, J = 8.7 Hz, 1H), 7.50 (t, J = 7.24 Hz, 2H), 7.37–7.44 (m, 1H), 7.20–7.32 (m, 1H), 6.94 (t, J = 6.9 Hz, 1H); TOF EI-MS: 320.3632 $[M]^+$.

*3-Iodo-2-naphthalenylindolizine (**2**).* pale yellow solid, M.P. 150–152 °C; ^{1}H NMR (400 MHz, $CDCl_3$, 25 °C, TMS) δ 8.24 (d, J = 6.9 Hz, 1H), 8.07 (d, J = 6.9 Hz, 2H), 7.63 (d, J = 8.7 Hz, 1H), 7.49 (t, J = 7.4 Hz, 2H), 7.37–7.44 (m, 1H), 7.20–7.32 (m, 1H), 6.94 (t, J = 6.9 Hz, 1H); TOF EI-MS: 369.9746 $[M]^+$.

General procedure for the Suzuki reaction. To a mixture of 3-iodo-2-phenylindolizine **1** (0.96 g, 3 mmol) and $Pd(PPh_3)_4$ (120 mg, 0.1 mmol) in 1,2-dimethoxyethane (DME, 16 mL) was added 1,4-benzenediboronic acid (0.2 g, 1.27 mmol) followed by the addition of sodium hydroxide (0.16 g, 4 mmol) in water (8 mL). The reaction mixture was refluxed at 85 °C for 40 h under argon. Then the mixture was poured into water (40 mL). The aqueous solution was extracted with dichloromethane (30 mL × 3). The combined organic extracts were washed with water (50 mL) and brine (50 mL). The dichloromethane solution was

dried over sodium sulfate, and the filtrate was evaporated *in vacuo*. The residue was subjected to column chromatography on alumina (solvent: dichloromethane) to obtain **PPI** (0.87 mmol; 57%).

1,4-Di-3′-(2′-phenylindolizyl)-benzene (***PPI***). pale yellow solid; ^{1}H NMR (400 MHz, $CDCl_3$, 25 °C, TMS) δ 8.15 (d, J = 6.88 Hz, 4H), 7.84 (d, J = 7.44 Hz, 4H), 7.72 (q, J_1 = 8.24 Hz, J_2 = 1.68 Hz, 8H), 7.65 (s, 8H), 7.35 (m, 16H), 6.90 (t, J = 6.52 Hz, 4H); ^{13}C NMR ($CDCl_3$, 100 MHz): δ 148.5, 138.2, 137.7, 133.0, 129.3, 129.2, 128.7, 128.0, 127.5, 126.2, 116.8, 114.6; TOF EI-MS: calcd. for $C_{32}H_{22}N_4$ 462.18, found 462.1678 $[M]^+$.

1,4-Di-3′-(2′-naphthalenylindolizyl)-benzene (***PNI***). pale yellow solid; ^{1}H NMR (400 MHz, $CDCl_3$, 25 °C, TMS) δ 8.30 (s, 2H), 8.18 (d, J = 6.88, 2H), 7.80 (m, 10H) 7.68 (s, 4H), 7.47 (m, 4H), 7.30 (t, J = 7.32, 2H), 6.87 (t, J = 6.32, 2H); ^{13}C NMR ($CDCl_3$, 100 MHz): δ 148.7, 138.7, 133.8, 133.2, 132.5, 129.5, 128.5, 128.1, 127.8, 127.7, 127.4, 126.8, 117.8, 115.6; TOF EI-MS: calcd. for $C_{40}H_{26}N_4$ 562.22, found 562.2174 $[M]^+$.

3-(4,4′-Biphenyl)-2-diphenylindolizine (***BPPI***). pale yellow solid; ^{1}H NMR (400 MHz, $CDCl_3$, 25 °C, TMS) δ 8.08 (d, J = 6.92 Hz, 2H), 7.87 (d, J = 8.24 Hz, 4H), 7.74 (q, J_1 = 6.76 Hz, J_2 = 1.6 Hz, 6H), 7.60 (d, J = 8.28 Hz, 4H), 7.31 (m, 8H), 6.81 (t, J = 8.17 Hz, 2H); ^{13}C NMR ($CDCl_3$, 100 MHz): δ 145.1, 142.9, 140.6, 134.2, 131.4, 129.5, 128.5, 128.4, 128.2, 127.8, 125.0, 123.4, 120.7, 117.8, 112.6; TOF EI-MS: calcd. for $C_{38}H_{26}N_4$ 538.22, found 538.1967 $[M]^+$.

3-(4,4′-Biphenyl)-2-dinaphthalenylindolizine (***BPNI***). pale yellow solid, ^{1}H NMR (400 MHz, $CDCl_3$, 25 °C, TMS) δ 8.35 (s, 2H), 8.14 (d, J = 6.92 Hz, 2H), 7.89 (d, J = 8.08 Hz, 4H), 7.80 (k, J_1 = 7.7 Hz, J_2 = 3.32 Hz, 6H), 7.75 (t, J = 1.52 Hz, 4H), 7.65 (d, J = 8.12 Hz, 4H), 7.45 (q, J_1 = 6.6 Hz, J_2 = 3.56 Hz, 4H), 7.31 (d, J = 6.52 Hz, 2H), 6.85 (s, J = 6.89 Hz, 2H); ^{13}C NMR ($CDCl_3$, 100 MHz): δ 147.3, 141.8, 135.0, 129.9, 129.4, 128.7, 128.4, 128.1, 127.5, 127.3, 124.9, 124.2, 123.4, 120.7, 120.0; TOF EI-MS: calcd. for $C_{46}H_{30}N_4$ 638.25, found 638.2088 $[M]^+$.

1,3,5-Tri[4-3′-(2′-naphthalenylindolizyl)phenyl]benzene (***p-TPPNI***). pale yellow solid; ^{1}H NMR (400 MHz, $CDCl_3$, 25 °C, TMS) δ 8.39 (s, 3H), 8.16 (d, J = 6.88 Hz, 3H), 8.06 (s, 3H), 7.98 (d, J = 8.16 Hz, 9H), 7.82 (m, 6H), 7.75 (m, 6H), 7.68 (d, J = 8.2 Hz, 6H), 7.46 (m, 6H), 7.39 (t, J = 7.53 Hz, 3H), 7.30 (m, 3H), 6.92 (t, J = 8.13 Hz, 3H); ^{13}C NMR ($CDCl_3$, 100 MHz): δ 145.0, 142.8, 142.0, 141.9, 134.1, 134.1, 130.7, 130.3, 129.9, 129.7, 128.5, 128.5, 128.4, 127.9, 127.8, 125.5, 125.1, 123.4, 120.9, 117.8, 112.7; MALDI-TOF MS: calcd. for $C_{75}H_{48}N_6$ 1032.39, found 1032.369 $[M]^+$.

1,3,5-Tri[3-3′-(2′-phenylindolizyl)phenyl]benzene (***m-TPPPI***). pale yellow solid; ^{1}H NMR (400 MHz, $CDCl_3$, 25 °C, TMS) δ 8.04 (d, J = 6.88 Hz, 3H), 7.76 (d, J = 7.88 Hz, 3H), 7.71 (m, 12H), 7.65 (t, J = 7.72 Hz, 3H), 7.52 (d, J = 7.56 Hz, 3H), 7.26 (m, 12H), 7.15 (t, J = 7.24 Hz, 3H), 6.80 (t, J = 7.37 Hz, 3H); ^{13}C NMR ($CDCl_3$, 100 MHz): δ 152.0, 146.8, 141.3, 140.3, 139.9, 137.9, 137.7, 129.9, 128.4, 127.9, 127.5, 127.1, 126.9, 126.7, 126.5, 126.0, 123.5, 123.2, 120.5, 120.3, 119.9, 119.6, 109.9, 109.7; MALDI-TOF MS: calcd. for $C_{63}H_{42}N_6$ 882.35, found 882.322 $[M]^+$.

Device fabrication. OLEDs were fabricated on patterned ITO-coated glass substrates with a sheet resistance of 30 Ω sq^{-1}. The substrates were cleaned with Decon 90, rinsed in de-ionized water, dried in an oven, and finally exposed to UV-ozone for about 25 min. The ITO substrates were then immediately transferred into a deposition chamber with a base pressure of 1×10^{-6} mbar. Organic layers were sequentially deposited at a rate of 0.1–0.2 nm s^{-1} by conventional vapor vacuum deposition. The Al cathode was then prepared by evaporation of Al after LiF of 1.5 nm was deposited.

Acknowledgements

This work was supported by National High-tech R&D Program of China (863 Program) (Grant No. 2011AA03A110), National Natural Science Foundation of China (Grant No. 50825304, 51033007, 51103169, 51128301) and Beijing Natural Science Foundation (Grant No. 2111002), P. R. China.

References

1 G. Schwartz, S. Reineke, T. C. Rosenow, K. Walzer and K. Leo, *Adv. Funct. Mater.*, 2009, **19**, 1319.
2 Y. Sun, N. C. Giebink, H. Kanno, B. Ma, M. E. Thompson and S. R. Forrest, *Nature*, 2006, **440**, 908.
3 J. Kido, K. Hongawa, K. Okuyama and K. Nagai, *Appl. Phys. Lett.*, 1994, **64**, 815.
4 J. Kido, H. Shionoya and K. Nagai, *Appl. Phys. Lett.*, 1995, **67**, 2281.
5 B. W. D'Andrade and S. R. Forrest, *J. Appl. Phys.*, 2003, **94**, 3101.
6 B. W. D'Andrade, R. J. Holmes and S. R. Forrest, *Adv. Mater.*, 2004, **16**, 624.
7 S. Tokito, T. Iijima, T. Tsuzuki and F. Sato, *Appl. Phys. Lett.*, 2003, **83**, 2459.
8 (*a*) R. J. Holmes, B. W. D'Andrade, S. R. Forrest, X. Ren, J. Li and M. E. Thompson, *Appl. Phys. Lett.*, 2003, **83**, 3818; (*b*) S. J. Yeh, M. F. Wu, C. T. Chen, Y. H. Song, Y. Chi, M. H. Ho, S. F. Hsu and C. H. Chen, *Adv. Mater.*, 2005, **17**, 285; (*c*) C. S. K. Mak, A. Hayer, S. I. Pascu, S. E. Watkins, A. B. Holmes, A. Kohler and R. Friend, *Chem. Commun.*, 2002, 4708; (*d*) X. Zhang, C. Jiang, Y. Mo, Y. Xu, H. Shi and Y. Cao, *Appl. Phys. Letter.*, 2006, **88**, 051116; (*e*) L. L. Wu, C. H. Yang, I. W. Sun, S. Y. Chu, P. C. Kao and H. H. Huang, *Organometallics*, 2007, **26**, 2017; (*f*) P. I. Shih, C. H. Chien, C. Y. Chuang, C. F. Shu, C. H. Yang, J. H. Chen and Y. Chi, *J. Mater. Chem.*, 2007, **17**, 1692; (*g*) L. Q. Chen, H. You, C. L. Yang, D. G. Ma and J. G. Qin, *Chem. Commun.*, 2007, 1352; (*h*) E. Orselli, G. S. Kottas, A. E. Konradsson, P. Coppo, R. Frohlich, L. De Cola, A. van Dijken, M. Buchel and H. Borner, *Inorg. Chem.*, 2007, **46**, 11082.
9 C. C. Chi, C. L. Chiang, S. W. Liu, H. Yueh, C. T. Chen and C. T. Chen, *J. Mater. Chem.*, 2009, **19**, 5561.
10 (*a*) S. J. Yeh, C. T. Chen, Y. H. Song, Y. Chi and M. H. Ho, *J. Soc. Inf. Disp.*, 2005, **13**, 857; (*b*) R. J. Holmes, S. R. Forrest, T. Sajoto, A. Tamayo, P. I. Djurovich, M. E. Thompson, J. Books, Y. J. Tung, B. W. D'Andrade, M. S. Weaver, R. C. Kwong and J. J. Brown, *Appl. Phys. Lett.*, 2005, **87**, 243507; (*c*) C. H. Yang, Y. M. Cheng, Y. Chi, C. J. Hsu, F. C. Fang, K. T. Wong, P. T. Chou, C. H. Chang, M. H. Tsai and C. C. Wu, *Angew. Chem., Int. Ed.*, 2007, **46**, 2418; (*d*) C. F. Chang, Y. M. C heng, Y. Chi, Y. C. Chiu, C. C. Lin, G. H. Lee, P. T. Chou, C. C. Chen, C. H. Chang and C. C. Wu, *Angew. Chem., Int. Ed.*, 2008, **47**, 4542.
11 (*a*) A. B. Chwang, M. Hack and J. L. Brown, *J. Soc. Inf. Disp.*, 2005, **13**, 481; (*b*) M. S. Weaver, R. C. Kwong, V. A. Adamovic, M. Kack and J. J. Brown, *J. Soc. Inf. Disp.*, 2006, **14**, 449.
12 (*a*) D. A. Lerner, P. M. Horowitr and E. M. Evleth, *J. Phys. Chem.*, 1977, **81**, 1; (*b*) J. Catakn, E. Mena, F. Fabero and F. A. Guerri, *J. Phys. Chem.*, 1992, **96**, 3.

13 S. Y. Takizawa, J. I. Nishida, T. Tsuzuki, S. Tokito and Y. Yamashita, *Inorg. Chem.*, 2007, **46**, 10.
14 J. Huang, W. J. Hou, J. H. Li, G. Li and Yang Yang, *Appl. Phys. Lett.*, 2006, **89**, 133509.
15 H. Sasabe, E. Gonmori, T. Chiba, Y. J. Li, D. Tanaka, S. J. Su, T. Takeda, Y. J. Pu, K. I. Nakayama and J. Kido, *Chem. Mater.*, 2008, **20**, 5951.
16 S. J. Su, D. Tanaka, Y. J. Li, H. Sasabe, T. Takeda and J. Kido, *Org. Lett.*, 2008, **10**, 5.
17 (*a*) Z. G. Hu, J. Liu, G. A. Li and Z. B. Dong, *J. Chem. Res.*, 2003, 778; (*b*) H. N. Hu, A. J. Zhang, L. S. Ding, X. X. Lei and L. X. Zhang, *J. Chem. Res.*, 2007, **2007**, 720; (*c*) S. S. Elmorsy, A. Pelter and K. Smtth, *Tetrahedron Lett.*, 1991, **32**, 4175; (*d*) J. Pang, Y. Tao, S. Freiberg, X. P. Yang, M. D'Iorio and S. Wang, *J. Mater. Chem.*, 2002, **12**, 206; (*e*) J. Palomero, J. A. Mata, F. Gonzalez and E. Peris, *New J. Chem.*, 2002, **26**, 291.
18 (*a*) I. G. C. Coutts, H. R. Goldschmid and O. C. Musgrave, *J. Chem. Soc. (C).*, 1970, 488; (*b*) J. J. Michels, M. J. Connell, P. N. Taylor and J. S. Wilson, *Chem.–Eur. J.*, 2003, **9**, 6167; (*c*) V. Diemer, H. Chaumeil, A. Defoin, P. Jacques and C. Carre, *Tetrahedron Lett.*, 2005, **46**, 47370; (*d*) C. Coudret, *Synth. Commun.*, 1996, **26**, 3543.
19 C. Enguehard, J. L. Renou, V. Collot, M. Hervet, S. Rault and A. Gueiffier, *J. Org. Chem.*, 2000, **65**, 6572.
20 P. Schrogel, A. Tomkeviciene, P. Strohriegl, S. T. Hoffmann, A. Kohler and C. Lennartz, *J. Mater. Chem.*, 2011, **21**, 2266.
21 (*a*) W. H. Melhuish, *J. Phys. Chem.*, 1961, **65**, 229; (*b*) N. O. Petersenr, R. Gratton and E. M. Pisters, *Can. J. Chem.*, 1987, **65**, 238.
22 (*a*) C. H. Huang, F. Y. Li, W. Huang, *Introduction to Organic Light-Emitting Materials and Devices*, Fudan University Press, Shanghai, 2005; (*b*) A. J. Bard and L. R. Faulkner, *Electrochemical analysis methods*, Chemical Industry Press, Beijing, 1995; (*c*) M. Sonntag and P. Strohriegl, *Chem. Mater.*, 2004, **16**, 4736; (*d*) D. Russell, R. Meyer, N. Jubran, Z. Tokarski, R. Moudry and K. Law, *J. Electroanal. Chem.*, 2004, **567**, 19.
23 C. C. Chi, C. L. Chiang, S. W. Liu, H. Yueh, C. T. Chen and C. T. Chen, *J. Mater. Chem.*, 2009, **19**, 5561.
24 S. L. Gong, Y. B. Zhao, M. Wang, C. L. Yang, C. Zhong, J. G. Qin and D. G. Ma, *Chem.–Asian J.*, 2010, **5**, 2093.
25 Y. Wei and C. T. Chen, *J. Am. Chem. Soc.*, 2007, **129**, 7478.
26 W. Y. Hung, L. C. Chi, W. J. Chen, Y. M. Chen, S. H. Chou and K. T. Wong, *J. Mater. Chem.*, 2010, **20**, 10113.
27 A. Endo and C. Adachi, *Chem. Phys. Lett.*, 2009, **483**, 224.
28 Y. T. Tao, Q. Wang, Y. Shang, C. L. Yang, L. Ao, J. G. Qin, D. G. Ma and Z. G. Shuai, *Chem. Commun.*, 2009, 77.

